Neuropharmacology 234 (2023) 109544

Contents lists available at ScienceDirect

Neuropharmacology

journal homepage: www.elsevier.com/locate/neuropharm

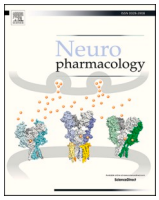

Neurotensin receptor 1-biased ligand attenuates neurotensin-mediated excitation of ventral tegmental area dopamine neurons and dopamine release in the nucleus accumbens

Sarthak M. Singhal [a], Vivien Zell [a], Lauren Faget [a], Lauren M. Slosky [b], Lawrence S. Barak [c], Marc G. Caron [d], Anthony B. Pinkerton [e,1], Thomas S. Hnasko [a,f,*]

[a] Department of Neurosciences, University of California San Diego, La Jolla, CA, USA
[b] Department of Pharmacology, University of Minnesota, Minneapolis, MN, USA
[c] Department of Cell Biology, Duke University, Durham, NC, USA
[d] Departments of Cell Biology, Neurobiology and Medicine, Duke University, Durham, NC, USA
[e] Conrad Prebys Center for Chemical Genomics, Sanford Burnham Prebys Medical Discovery Institute, La Jolla, CA, USA
[f] Research Service, VA San Diego Healthcare System, San Diego, CA, USA

ARTICLE INFO

Handling Editor: M. Roberto

Keywords:
Neurotensin
Neurotensin receptor-1
Dopamine
D2 autoreceptor
Ventral tegmental area
Nucleus accumbens

ABSTRACT

Strong expression of the G protein-coupled receptor (GPCR) neurotensin receptor 1 (NTR1) in ventral tegmental area (VTA) dopamine (DA) neurons and terminals makes it an attractive target to modulate DA neuron activity and normalize DA-related pathologies. Recent studies have identified a novel class of NTR1 ligand that shows promising effects in preclinical models of addiction. A lead molecule, SBI-0654553 (SBI-553), can act as a positive allosteric modulator of NTR1 β-arrestin recruitment while simultaneously antagonizing NTR1 Gq protein signaling. Using cell-attached recordings from mouse VTA DA neurons we discovered that, unlike neurotensin (NT), SBI-553 did not independently increase spontaneous firing. Instead, SBI-553 blocked the NT-mediated increase in firing. SBI-553 also antagonized the effects of NT on dopamine D2 auto-receptor signaling, potentially through its inhibitory effects on G-protein signaling. We also measured DA release directly, using fast-scan cyclic voltammetry in the nucleus accumbens and observed antagonist effects of SBI-553 on an NT-induced increase in DA release. Further, in vivo administration of SBI-553 did not notably change basal or cocaine-evoked DA release measured in NAc using fiber photometry. Overall, these results indicate that SBI-553 blunts NT's effects on spontaneous DA neuron firing, D2 auto-receptor function, and DA release, without independently affecting these measures. In the presence of NT, SBI-553 has an inhibitory effect on mesolimbic DA activity, which could contribute to its efficacy in animal models of psychostimulant use.

1. Introduction

Neurotensin (NT) is a 13 amino acid neuropeptide abundantly expressed in brain (Schroeder et al., 2019; Woodworth et al., 2018a) and implicated in the pathophysiology of several neuropsychiatric disorders (Boules et al., 2014; Cáceda et al., 2006; St-Gelais et al., 2006). Central effects of NT are mediated in large part through its high affinity G protein-coupled receptor (GPCR), neurotensin receptor type 1 (NTR1) (Binder et al., 2001; Tschumi and Beckstead, 2019). Expression of NTR1 on the majority of dopamine (DA) cells in ventral tegmental area (VTA) (Alexander and Leeman, 1998; Palacios and Kuhar, 1981; Quirion et al., 1985; Woodworth et al., 2017, 2018b), as well as presynaptically on DA terminals in the nucleus accumbens (NAc) (Dilts and Kalivas, 1989; Fawaz et al., 2009; Pickel et al., 2001; Schotte and Leysen, 1989), suggest regulation of DA neuron excitability and release by NT. This association of NTR1 with mesolimbic circuitry and the influence of NT signaling on behaviors linked to behavioral disorders make NTR1 an attractive target for drug development (Binder et al., 2001; Ferraro et al., 2016; Geisler et al., 2006; Torruella-Suárez and McElligott, 2020).

Stimulation of NTR1 can activate G-protein signaling and the recruitment of β-arrestins leading to receptor internalization and desensitization (Besserer-Offroy et al., 2017; Huang et al., 2020; Slosky

* Corresponding author. Department of Neurosciences, University of California San Diego, La Jolla, CA, USA.
E-mail address: thnasko@health.ucsd.edu (T.S. Hnasko).
[1] Present address: Boundless Bio, Inc., San Diego, CA, USA.

https://doi.org/10.1016/j.neuropharm.2023.109544
Received 2 December 2022; Received in revised form 29 March 2023; Accepted 10 April 2023
Available online 11 April 2023
0028-3908/Published by Elsevier Ltd.

et al., 2020). In addition to neuromodulation of the DA system, activation of NTR1 can affect other physiological functions like regulation of body temperature, blood pressure, food intake and motor coordination (Boules et al., 2013; Pettibone et al., 2002; Remaury et al., 2002; Richelson et al., 2003), likely due to engagement of both G-proteins and β-arrestins, which can have distinct effects on cellular and physiological functions (Reiter et al., 2012; Smith and Rajagopal, 2016). Hence, biased NTR1 ligands with effects on specific intracellular signaling pathways need to be developed and tested. SBI-0654553 (SBI-553) was developed as an optimized non-peptide ligand of NTR1 with good oral bioavailability and brain penetration in rodents, and was shown to bias NTR1 signaling towards β-arrestin recruitment while antagonizing G-protein activation (Pinkerton et al., 2019). Moreover, SBI-553 attenuated the reinforcing effects of psychostimulants without causing side effects associated with balanced NTR1 agonism (Slosky et al., 2020), placing it as a promising candidate for therapeutic development. However, little is known about how SBI-553 influences cellular function in the brain. Therefore, we here investigated how SBI-553 affects mesolimbic DA function.

NT can directly excite VTA DA neurons through NTR1-coupled activation of G_q and recruitment of downstream signaling pathways, leading to an increase in intracellular calcium (Besserer-Offroy et al., 2017; St-Gelais et al., 2004; Tschumi and Beckstead, 2019). NT can also disinhibit VTA DA neurons through NTR1-mediated inhibition of the G_i-coupled type-2 DA auto-receptors (D2R) (Jomphe et al., 2006; Shi and Bunney, 1992; Werkman et al., 2000). Furthermore, NT can enhance DA release by acting on presynaptic DA terminals in the NAc, possibly through inhibition of D2R (Fawaz et al., 2009). However, how SBI-553 acting as an antagonist of G protein signaling through NTR1, or as a positive allosteric modulator of β-arrestin signaling through NTR1 or acting through both mechanisms simultaneously to affect DA neuron function has not been established. Here, we report that SBI-553 blunted NT effects on spontaneous DA neuron firing, D2R function, and DA release, without independently affecting these measures in the absence of NT. Overall, our results suggest an NT-dependent inhibitory effect of SBI-553 on DA function, which could contribute to observed behavioral or therapeutic effects of this ligand.

2. Material and methods

2.1. Animals

Mice were bred at the Veterans Affairs San Diego Healthcare System (VASDHS) or University of California San Diego (UCSD) and group housed on a 12-h light/dark cycle with ad libitum access to pelleted chow and water. Initial breeders DAT-Cre (Slc6a3, Stock: 006660), Ai14 tdTomato reporter (Gt(ROSA)26Sor, Stock: 007914) and C57 (C57Bl/6J, Stock: 000664) were obtained from Jackson laboratories. Heterozygous mice carrying one copy of DAT-Cre and one copy of the tdTomato reporter were used for slice electrophysiology and FSCV experiments. C57 mice were used for fiber photometry. Male and female mice were used for all experiments. All animal procedures were approved by the UCSD or VASDHS Institutional Animal Care and Use Committees.

2.2. Cell-attached recordings for testing effects of NT and SBI-553 on VTA DA neuron firing

On day of experiments, mice (age 4–8 weeks) were deeply anesthetized with sodium pentobarbital (200 mg/kg i.p.; Virbac) and perfused intracardially with 10 ml ice-cold sucrose artificial cerebrospinal fluid (ACSF) containing (in mM): 75 sucrose, 87 NaCl, 2.5 KCl, 7 $MgCl_2$, 0.5 $CaCl_2$, 1.25 NaH_2PO_4, 25 $NaHCO_3$ and continuously bubbled with carbogen (95% O_2 + 5% CO_2). Brains were extracted and sectioned to obtain 200-μm coronal slices of VTA in sucrose-ACSF using a Leica Vibratome (VT 1200). Slices were transferred to a recovery chamber containing ACSF (in mM): 126 NaCl, 2.5 KCl, 1.2 $MgCl_2$, 2.4 $CaCl_2$, 1.4 NaH_2PO_4, 25 $NaHCO_3$ and 11 glucose, continuously bubbled in carbogen. After at least 45 min recovery, slices were transferred to a recording chamber continuously perfused with ACSF (2–3 ml/min) maintained at 31 °C. Patch pipettes (3.5–5.5 MΩ) were pulled from borosilicate glass (King Precision Glass) using a micro-pipette puller (Narishige, PC-10) and filled with ACSF for cell-attached recordings. tdTomato labelled VTA DA neurons were identified through epifluorescence imaging using a 40X water-immersion objective, X-Cite Series 120Q light source (Lumen Dynamics) and a Zeiss filter set, and visually guided patch recordings were made using infrared-differential interference contrast (IR-DIC) illumination (Axiocam MRm, Examiner.A1, Zeiss). Action potentials (APs) were recorded in cell-attached configuration under voltage-clamp (Multiclamp 700B amplifier, Axon Instruments), filtered at 2 kHz, digitized at 10 kHz (Axon Digidata 1550, Axon Instruments) and collected on-line using Clampex v10 software (Molecular Devices). AP frequency was averaged over a period of 120 s before, and during bath application of the compounds. DMSO or H_2O stock solutions of drugs at 1 mM were diluted in ACSF and bath applied at the following concentrations, NT (in nM): 3.5, 35, 100 & 350; SBI-553 (in μM): 1, 10 & 100.

2.3. Cell-attached recordings for testing NT and SBI-553 effects on D2R inhibition in VTA DA neurons

Using 6-12 week-old mice, 200-μm coronal sections of VTA were obtained as above using ice-cold N-methyl D-glucamine (NMDG)-ACSF containing (in mM): 92 NMDG, 2.5 KCl, 1.25 NaH_2PO_4, 30 $NaHCO_3$, 20 HEPES, 25 D-glucose, 2 thiourea, 5 Na-ascorbate, 3 Na-pyruvate, 0.5 $CaCl_2$ and 10 $MgSO_4$. Sections were transferred to a recovery chamber containing 150 mL of preheated (32–34 °C), NMDG-ACSF. Increasing volumes of 2 M Na^+ spike-in solution were added to the recovery chamber in 5-min increments to achieve a controlled rate of Na^+ reintroduction (Ting et al., 2018), following which they were transferred to ACSF at room temperature containing (in mM): 115 NaCl, 2.5 KCl, 1.23 NaH_2PO_4, 2 $MgSO_4$, 10 D-glucose, 2 $CaCl_2$, 26 $NaHCO_3$, 2 thiourea, 5 Na-ascorbate and 3 Na-pyruvate. Slices were allowed to equilibrate for at least 1 h, then transferred to a recording chamber and perfused continuously at a rate of 1.5–2 ml/min with ACSF maintained at 31 °C that contained (in mM): 125 NaCl, 2.5 KCl, 1.2 NaH_2PO_4, 2 $MgSO_4$, 12.5 D-glucose, 2 $CaCl_2$ and 26 $NaHCO_3$. All solutions were continuously bubbled with carbogen. Patch pipettes (6–7 MΩ) prepared from thin-walled borosilicate glass capillaries (Sutter Instruments) were used to make patch-clamp recordings from visualized tdTomato$^+$ VTA DA neurons. Effects on firing frequency were assessed in cell-attached mode in voltage clamp (V_h set to −35 to −40 mV so that holding current was zero) using pipettes that were filled with (in mM): 145 NaCl, 2.5 KCl, 2 $CaCl_2$, 1 $MgCl_2$, 0.7 NaH_2PO_4 and 10 HEPES, adjusted to pH of 7.3 and 280 mOsm. Data was collected at 20 kHz, lowpass filtered at 1 kHz and analyzed using Clampfit v10.7 software.

To study effects of D2R signaling in VTA DA cells, D2R agonist quinpirole (quin) was bath applied for 3 min after baseline recording of spontaneous firing. To test effects of NT on D2R function, NT was bath applied for 28 min followed by washout, and quin was applied 15 min after start of NT application for 3 min. Experiments involving SBI-553, NT and quin had the following design: SBI-553 was bath applied for 43 min followed by washout, NT was bath applied 15 min after start of SBI-553 application for 28 min and quin was bath applied 15 min after start of NT application for 3 min. Finally, for experiments investigating effects of SBI-553 on D2R function, SBI-553 was bath applied for 28 min followed by washout and quin was applied 15 min after start of SBI-553 application for 3 min. To avoid potential confound of 'basement' effects of quin on DA neuron inhibition, cells with very low baseline firing frequency (<1 Hz) were discarded without performing subsequent pharmacology. Firing was assessed in 30-s bins and quin response for a cell was calculated as the largest change in AP firing frequency during its 3-min application period compared to the mean of the 2-min period

before its application.

Quin stock solution of 2 mM was diluted in ACSF and applied at 2 μM, NT stock solution of 200 μM was diluted in ACSF and applied at 10 nM and SBI-553 HCl stock solution of 2 mM in 1.67% DMSO was diluted in ACSF and applied at 10 μM. (-) Quinpirole hydrochloride and NT were purchased from Tocris and Sigma-Aldrich respectively; SBI-553 HCl was synthesized at Sanford Burnham Prebys Medical Research Institute as described (Pinkerton et al., 2019).

2.4. FSCV recordings

Coronal brain sections of the NAc (300 μm) were prepared from mice (6–12 weeks) as described in section 2.3. Carbon fiber electrodes (CFE) were fabricated from 7-μm diameter carbon fiber (GoodFellow) inserted in a borosilicate glass capillary (1 mm/0.5 mm, A-M systems) and pulled to seal the pipette around the carbon fiber using a micro-pipette puller (Narishige, PC-10). Exposed fiber was cut to a length of 50–150 μm. Electrodes were then filled with 3 M KCl and lowered into the recording chamber with oxygenated ACSF perfused continuously at 1.5–2 ml/min at 31 °C. A triangular voltage ramp (−0.4V to +1.3V) was applied to the electrode at 60 Hz at a rate of 400 V/s for 10–15 min and resulting background current was allowed to stabilize, following which the voltage ramp waveform was applied at 10 Hz for the rest of the experiment. The CFE along with a concentric bipolar stimulator (FHC Inc) were lowered in to the ventral medial NAc shell, separated by 100–150 μm, visually guided using IR-DIC microscopy. Current transients were evoked using trains of electrical stimulation (10 Hz, 6 pulses, 0.2 ms pulse width, 300 μA current intensity) generated using a A365 stimulus isolator (World Precision Instruments), applied every 3 min, and controlled by TarheelCV software. Background subtracted cyclic voltammograms had peak oxidation potential of 600–700 mV characteristic of DA. The peak of DA current in response to stimulation was measured and plotted over time as DA concentration after calibration of CFE to 1 μM DA (Alfa Aesar A11136) prepared fresh daily. Data was collected and analyzed using TarheelCV.

SBI-553 (stock solution of 2 mM in 1.67% DMSO, diluted in ACSF and applied at 10 μM) or its vehicle alone were bath applied for 35 min after baseline recordings followed by washout, and NT was bath applied 15 min after start of vehicle or SBI-553 application for 20 min. NT stock solution of 200 μM was diluted in ACSF and applied at 100 nM. NT response was calculated as the average change in peak current 5 min after start of application of NT, for the next 9 min, compared to average peak current during 10 min before start of NT application. Time graphs were baseline subtracted to average the 5 data points before bath application of drug or vehicle.

2.5. Stereotactic surgery

For intracranial injections, mice (7–10 weeks) were deeply anesthetized with isoflurane and placed into a stereotaxic apparatus (Kopf). 500 nl of AAV5-CAG-dLight1.1 (8.1×10^{12} GC/ml, Addgene 11067) was infused unilaterally into the NAc (ML = −0.6, AP = +1.3, DV = −4.45; mm relative to Bregma) using custom-made glass pipettes (~25 μm aperture diameter) and a Nanoject III (Harvard Apparatus) at a rate of 10 nl/s with 1-s pulse and 5-s inter-pulse interval. The glass pipettes were held in place for 5 min after infusion before retracted. Following AAV infusion, a 1.25 mm-diameter metal ferrule, 6 mm long, 400 μm core, 0.48 NA optic fiber (Doric Lenses, Canada) was implanted in NAc (ML = −0.6, AP = +1.3, DV = −4.2; mm relative to Bregma) for fiber photometry recordings. Fibers were stabilized in place using dental cement (Lang dental) secured by two skull screws (Plastics One). Animals were administered with the analgesic carprofen (5 mg/kg s.c.; Rimadyl) after surgery, monitored daily and allowed to recover for 5–6 weeks before experiments began.

2.6. Fiber photometry recordings in vivo

Mice were habituated to handling for 6 days prior to recordings. On test days, mice were tethered with a fiber photometry optic fiber cable through a pigtailed rotary joint (DORIC) and allowed to freely explore an open field (50 × 50 cm) for 30 min while recording baseline signals. After 30 min, vehicle (3% DMSO in saline, i.p.) or SBI-553 (12 mg/kg, i.p.) dissolved in vehicle was injected; 15 min later, cocaine (20 mg/kg in saline, i.p.) was injected and recordings made for another 50 min. Vehicle or SBI-553 was injected in a counterbalanced manner across 2 test days (day 1 and day 3), with a day off between treatments (day 2 and day 4). One mouse was excluded due to repeated cable detachment during cocaine recording days. On day 5 all mice received SBI-553. Mice were tethered to the optic fiber cable, baseline signals recorded for 30 min, injected with vehicle for 15 min recording, then injected with SBI-553 and recorded for another 40 min. Locomotor activity was recorded and analyzed using automated video tracking system using AnyMaze software (Stoelting, CA). Cocaine hydrochloride was purchased from Sigma-Aldrich.

For fiber photometry recordings, dLight 1.1 was excited by amplitude-modulated signals from two light-emitting diodes (465- and 405-nm isosbestic control, DORIC) reflected off dichroic mirrors (6-port minicube, DORIC), delivered through an optic fiber. Signals were returned through the same optic fiber and acquired using a femtowatt photoreceiver (Newport), digitized at 1017 Hz, and recorded by a real-time signal processor (RZ5P, Tucker Davis Technologies). Event timestamps related to vehicle, SBI-553 and cocaine injections were digitized in Synapse software (Tucker Davis Technologies) by TTL inputs from AnyMaze. Signals were analyzed using custom-written MATLAB scripts. Data were detrended by regressing the isosbestic control signal (405 nm) on the sensor signal (465 nm) and then generating a fitted 405-nm signal using the linear model generated during the regression. However, 405 and 465 signals were analyzed and displayed separately after it was observed that SBI-553 independently affected the isosbestic control signal. Area under curve (AUC) was calculated for the sensor (465 nm) signal and locomotor activity after cocaine injections (minutes 46 through 90).

2.7. Histology

Following fiber photometry experiments, mice were deeply anesthetized with sodium pentobarbital (200 mg/kg; i.p.) and transcardially perfused with ~20 ml of phosphate buffered saline (PBS) followed by ~20 ml 4% paraformaldehyde (PFA) at a rate of 5–6 ml/min. Brains were extracted, post-fixed in 4% PFA at 4 °C overnight, and transferred to 30% sucrose in PBS for 48–72 h at 4 °C. Brains were flash frozen in isopentane and stored at -80 °C. 30-μm coronal sections were cut using a cryostat (CM3050S, Leica) and collected in PBS containing 0.01% sodium azide. For immunostaining, brain sections were gently rocked 3 × 5 min in PBS, 3 × 5 min in PBS containing 0.2% Triton X-100 (PBST) and blocked with 4% normal donkey serum (NDS) in PBST for 1 h at room temperature (RT). Sections were then incubated in primary antibody chicken anti-GFP (1:2000; Invitrogen A10262) added to 4% NDS block solution at 4 °C overnight. Following this, sections were rinsed 3 × 10 min with PBST and incubated in secondary antibody Alexa 488 donkey anti-chicken (1:400; Jackson ImmunoResearch) for 2 h at RT. Sections were washed 3 × 10 min with PBS, mounted on slides, and coverslipped with Fluoromount-G mounting medium (Southern Biotech) containing DAPI (0.5 μg/ml; Roche). Images were acquired using widefield epifluorescence (Zeiss AxioObserver) with a 5X objective with identical acquisition settings across slides. dLight expression and optic fiber placements were mapped onto corresponding coronal sections in the Paxinos Mouse Brain Atlas using Inkscape.

2.8. Statistical analysis

Statistical analysis was performed using GraphPad Prism v9. All data shown in time traces and bar plots represent mean ± SEM. Data were tested for normality using the Shapiro-Wilk test and appropriate parametric or non-parametric tests were used. Data was analyzed using Student's t-test or Wilcoxon test, one-way ANOVA with Tukey's post hoc test, or Friedmans test and repeated measures (RM) two-way ANOVA. Significance was set at $p < 0.05$.

3. Results

3.1. SBI-553 does not affect firing of VTA DA neurons but blocks NT-mediated activation

To test the effects of SBI-553 on DA neuron firing we performed cell-attached recordings from VTA DA neurons in mice expressing Cre-dependent tdTomato in dopamine transporter (DAT) expressing neurons (Fig. 1A). Bath application of NT significantly increased DA neuron firing when applied at 35 nM ($t_6 = 2.7$, $p = 0.03$), 100 nM ($p = 0.0005$, Wilcoxon test) and 350 nM ($p = 0.015$, Wilcoxon test), but not at 3.5 nM ($p = 0.12$, Wilcoxon test) (Fig. 1 A-E). In contrast, application of SBI-553 did not affect DA neuron firing: 1 μM, $t_6 = 1.8$, $p = 0.12$; 10 μM, $t_6 = 1.6$, $p = 0.17$; 100 μM, $t_3 = 1.3$, $p = 0.28$ (Fig. 1 F–I). However, pre-application of SBI-553 blocked the NT-mediated increase in firing ($p = 0.68$, Friedman test) (Fig. 1J).

3.2. SBI-553 blocks the ability of NT to oppose D2R signaling

NT also regulates excitability of VTA DA neurons through regulation of D2R signaling (Jomphe et al., 2006; Thibault et al., 2011). We therefore evaluated effects of NT and SBI-553 on the change in VTA DA neuron firing induced by the D2R agonist quinpirole (quin), using cell-attached recordings. We reasoned that if NT reduces D2R function through a G-protein-dependent pathway, then SBI-553 would oppose the ability of NT to suppress quin-mediated inhibition. On the other hand, if NT inhibits D2R function via recruitment of β-arrestin-dependent pathways, then SBI-553, a PAM of NTR1 β-arrestin recruitment, may enhance NT-mediated suppression of D2R signaling.

Bath application of quin decreased firing in all recorded VTA DA neurons (Fig. 2A and B). Pre-application of NT increased DA neuron firing (Fig. 2C), but also blunted the inhibitory effects of quin (Fig. 2C, F, G). Application of SBI-553 alone did not increase DA neuron firing (Fig. 2D and E), nor did SBI-553 block quin-mediated inhibition of DA neuron firing (Fig. 2E-G). However, SBI-553 did blunt the effects of NT on DA neuron firing (Fig. 2D), and on the NT-mediated inhibition of quin (Fig. 2D, F, G) (Main effect of treatment on quin-mediated inhibition; change in frequency: $F_{3,34} = 9.9$, $p < 0.0001$, percent change in frequency: $F_{3,34} = 8.3$, $p = 0.0003$). No differences in baseline firing across the four groups were detected ($F_{3,34} = 0.27$, $p = 0.85$) (Fig. 2H), suggesting similar properties for the cells sampled across the groups. These results suggest that SBI-553 can inhibit VTA DA neurons by blocking NT's ability to oppose D2R-mediated autoinhibition.

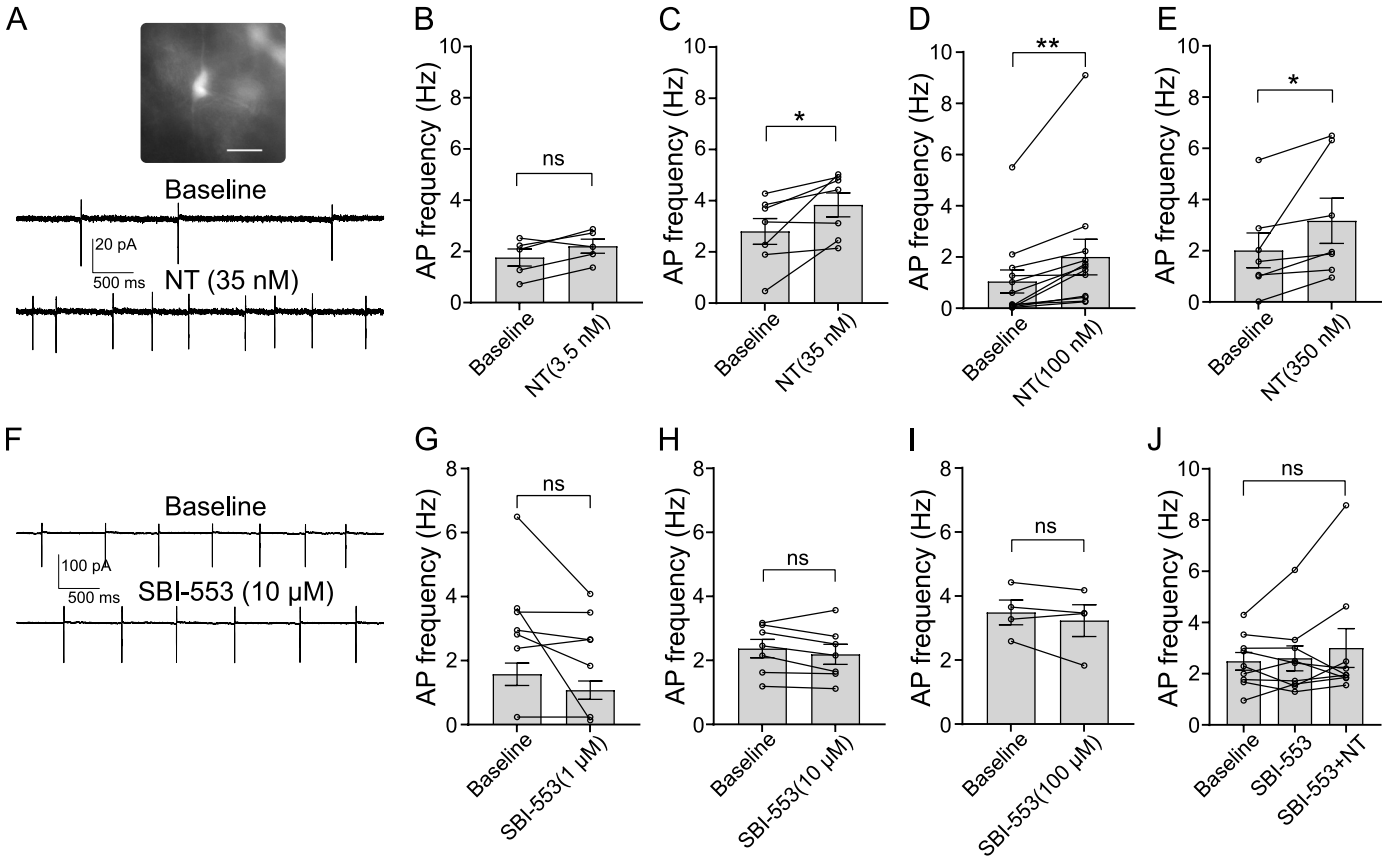

Fig. 1. SBI-553 does not alter DA neuron firing but blocks NT mediated activation of VTA DA neurons. **(A)** Example image (scale 25 μm) and cell-attached recording from a tdTomato-positive cell in VTA. Bath application of different concentrations of NT **(B)** 3.5 nM (n = 5), **(C)** 35 nM (n = 7), **(D)** 100 nM (n = 12) & **(E)** 350 nM (n = 7), increased firing of VTA DA neurons. NT responses were compared to their baseline using paired *t*-test or Wilcoxon test. *p < 0.05, **p < 0.005. **(F)** Example recording from a VTA DA cell showing no effects of SBI-553 (10 μM) on firing. Bath application of different concentrations of SBI-553 **(G)** 1 μM (n = 7), **(H)** 10 μM (n = 7) & **(I)** 100 μM (n = 4) did not affect firing of VTA DA cells; not significant (ns) by paired *t*-test. **(J)** Pre-application of SBI-553 (1 μM) blocked NT (100 nM)-mediated activation of VTA DA neurons (n = 9); Friedman test, p = 0.68.

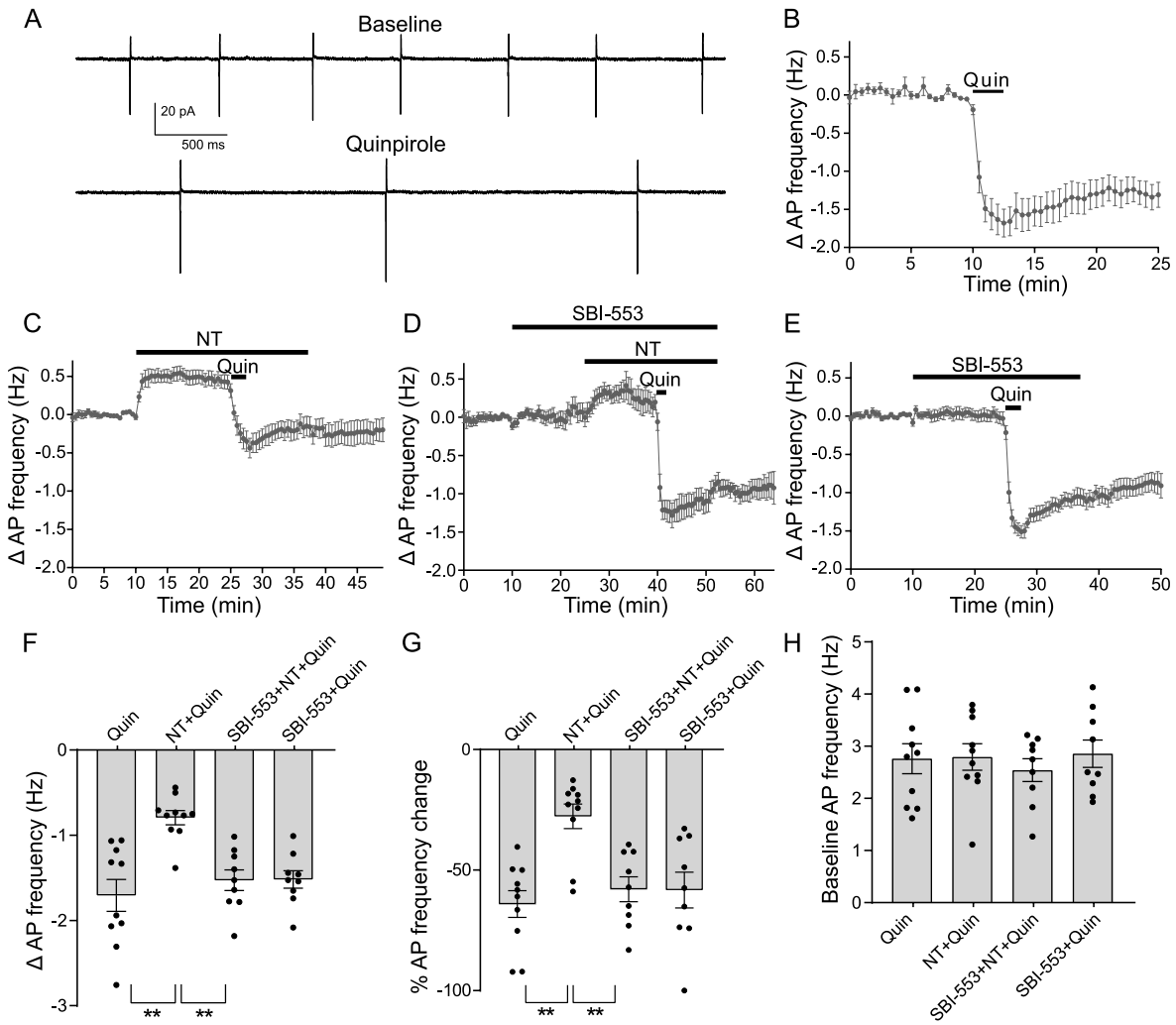

Fig. 2. SBI-553 inhibits effects of NT on D2R signaling in VTA DA neurons. **(A)** Example cell-attached recording from a VTA DA neuron showing **(B)** quin (2 μM)-induced reduction in firing (n = 10). Averaged traces showing effects on quin-induced inhibition following bath application of **(C)** NT (10 nM, n = 10), **(D)** SBI-553 (10 μM) plus NT (n = 9), or **(E)** SBI-553 (n = 9). **(F)** Change in action potential (ΔAP) from baseline represented in frequency (Hz) or **(G)** percent change (%) show that NT blunts quin-induced inhibition, and this effect of NT was blocked by SBI-553. One-way ANOVA with Tukey's post-hoc test, **p < 0.005. **(H)** Baseline firing rate was similar across groups; one-way ANOVA, p = 0.85.

3.3. SBI-553 blocks NT-mediated enhancement of evoked DA release in NAc

Short trains of electrical or optogenetic stimulation in NAc have been shown to activate D2Rs expressed on presynaptic terminals by local DA release (Phillips et al., 2002; Shin et al., 2017) and application of NT in the NAc shell was reported to enhance evoked DA release, potentially through inhibition of D2R signaling (Fawaz et al., 2009). We therefore hypothesized that, similar to its effects on DA neurons in VTA, SBI-553 would antagonize NT-mediated excitatory effects on DA release. To test this, we used FSCV to measure electrically evoked DA release in ventral medial NAc shell in mouse brain slices (Fig. 3A and B). We found that bath application of NT resulted in a small but significant enhancement in evoked DA release, which was inhibited by SBI-553 (change in DA: effect of time $F_{4.9,\ 187} = 3.9$, $p = 0.002$, effect of treatment $F_{1,\ 38} = 5.0$, $p = 0.03$, time × treatment interaction $F_{21,\ 798} = 2.9$, $p < 0.0001$; % change in DA: effect of time $F_{3.9,\ 148} = 4.0$, $p = 0.004$, effect of treatment $F_{1,\ 38} = 5.2$, $p = 0.03$, time × treatment interaction $F_{21,\ 798} = 3.8$, $p < 0.0001$; average of NT induced % change in DA: $t_{38} = 2.7$, $p = 0.01$) (Fig. 3C–E).

3.4. SBI-553 does not alter cocaine-evoked NAc DA release in vivo

To test whether SBI-553 independently affects basal and cocaine-evoked DA release in NAc, we treated mice with SBI-553 and/or cocaine over several test days (Fig. 4A) and used fiber photometry to record changes in fluorescence (F) of a genetically encoded DA sensor dLight 1.1 (Fig. 4B). Cocaine evoked the expected increase in DA release in NAc, observed as an increase in 465 nm F (Fig. 4C), however the cocaine-evoked increase was unchanged by pre-treatment with SBI-553 ($t_8 = 0.22$, $p = 0.83$) (Fig. 4D). Cocaine also induced the expected hyperlocomotion (Fig. 4E). While the onset of cocaine-induced locomotion may have been delayed by SBI-553 pretreatment (effect of time $F_{2.9,\ 46} = 13.5$, $p < 0.0001$, effect of treatment $F_{1,\ 16} = 0.0001$, $p = 0.99$; time × treatment interaction $F_{16,\ 256} = 1.4$, $p = 0.12$), cumulative locomotor activity was not changed by SBI-553 under these conditions ($t_8 = 0.01$, $p = 0.99$) (Fig. 4F). In the above recordings we also observed a small SBI-553-induced increase in F, particularly at 405 nm, prior to administration of cocaine (Fig. 4C). We confirmed this with a follow-on test where mice were given SBI-553 without subsequent cocaine (Fig. 4G), and for this reason we analyzed 465 nm unnormalized to isosbestic 405 nm F. Overall, these results suggest that SBI-553 does not acutely influence DA release, nor affect cocaine-evoked DA release in

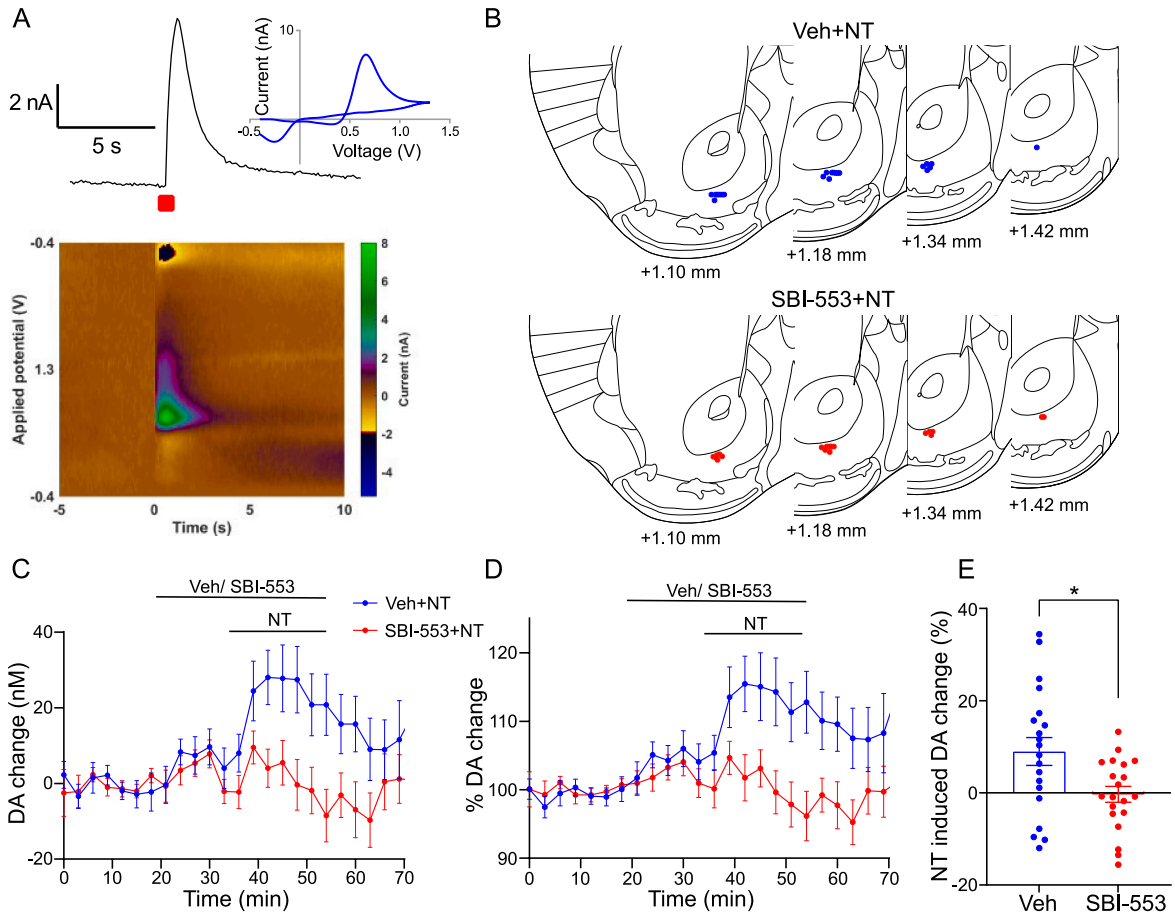

Fig. 3. SBI-553 inhibits NT-induced increase in evoked DA release in ventral medial NAc shell. **(A)** Example DA transient resulting from electrical stimulation in NAc (top) and corresponding voltammogram taken at the peak of DA transient (top). Color plot shows current measured at the electrode across entire range of applied potentials (bottom). Red square denotes electrical stimulation (6 pulses at 10 Hz). **(B)** Map of CFE recording sites. **(C)** DA transient evoked every 3 min plotted across time in the presence of vehicle (Veh) plus NT (100 nM) or SBI-553 (10 μM) plus NT (100 nM), as absolute change in concentration from baseline or **(D)** percent change from baseline. **(E)** Average percent change reveals NT-induced increase in evoked DA response is blocked by SBI-553, n = 20 recordings from 12 mice per group. Unpaired *t*-test, *p < 0.05.

NAc.

4. Discussion

In the current study, we report that SBI-553 antagonized NT effects on spontaneous firing and D2R function in VTA DA neurons, without independently affecting these measures. We also observed that SBI-553 blocked NT-mediated enhancement of evoked DA release in NAc. This is consistent with prior studies showing that activation of NTR1 increases DA neuron firing through G protein modulation of multiple cation channels, including a decrease in conductance of inwardly rectifying K^+ channels, activation of non-selective cation channels including transient receptor potential (TRP) channels, and activation of inositol triphosphate (IP3) receptors (Binder et al., 2001; St-Gelais et al., 2004; Stuhrman and Roseberry, 2015; Tschumi and Beckstead, 2019). NTR1-mediated inhibition of D2Rs in DA neurons is also mediated through recruitment of G_q-coupled protein kinase C or G_s-coupled protein kinase A, resulting in D2R phosphorylation and desensitization or internalization (Jomphe et al., 2006; Shi and Bunney, 1992; Thibault et al., 2011). Therefore, SBI-553 mediated antagonism of G protein signaling may be sufficient to explain its inhibitory effects on NT-mediated DA neuron excitation. However, it is also possible that SBI-553 potentiation of β-arrestin and subsequent NTR1 internalization (Slosky et al., 2020) contributes to the antagonistic effect we here observed.

NTR1 β-arrestin-mediated heterologous desensitization of D2R could also be a mechanism through which NT opposes D2R signaling. Indeed, NT's inhibitory effects on D2R function can occur through a G protein-independent mechanism (von Euler et al., 1991). However, it is unlikely that β-arrestin-dependent mechanisms acting alone could explain our results because SBI-553, acting as a PAM of β-arrestin signaling, would instead have potentiated rather than blocked the inhibitory effects of NT on D2R signaling. Moreover, by recruiting β-arrestins, SBI-553 should have directly inhibited D2R function in the absence of NT ligand, but this was not observed in our current study. Expression of NTR1 in midbrain DA neurons is also under developmental regulation (Woodworth et al., 2018b) and some midbrain DA neurons express other NT receptors, which could contribute to NT's effects independent of SBI-553's effects on NTR1 (Piccart et al., 2015; Sarret et al., 1998; Tschumi et al., 2022; Woodworth et al., 2018b).

Though the effect was variable across our FSCV recordings, we found that NT significantly enhanced DA release in NAc, corroborating previous studies (Reyneke et al., 1992). Although we did not test the mechanism underlying this effect, NT has been shown to regulate DA release in NAc through inhibition of D2R expressed on presynaptic DA terminals (Fawaz et al., 2009). NT has also been shown to increase spontaneous excitatory post-synaptic currents in cultured rat VTA DA neurons through inhibition of presynaptic D2Rs (Legault et al., 2002). Our observed NT-mediated increase in evoked DA release might thus be through negative regulation of presynaptic D2R, with SBI-553

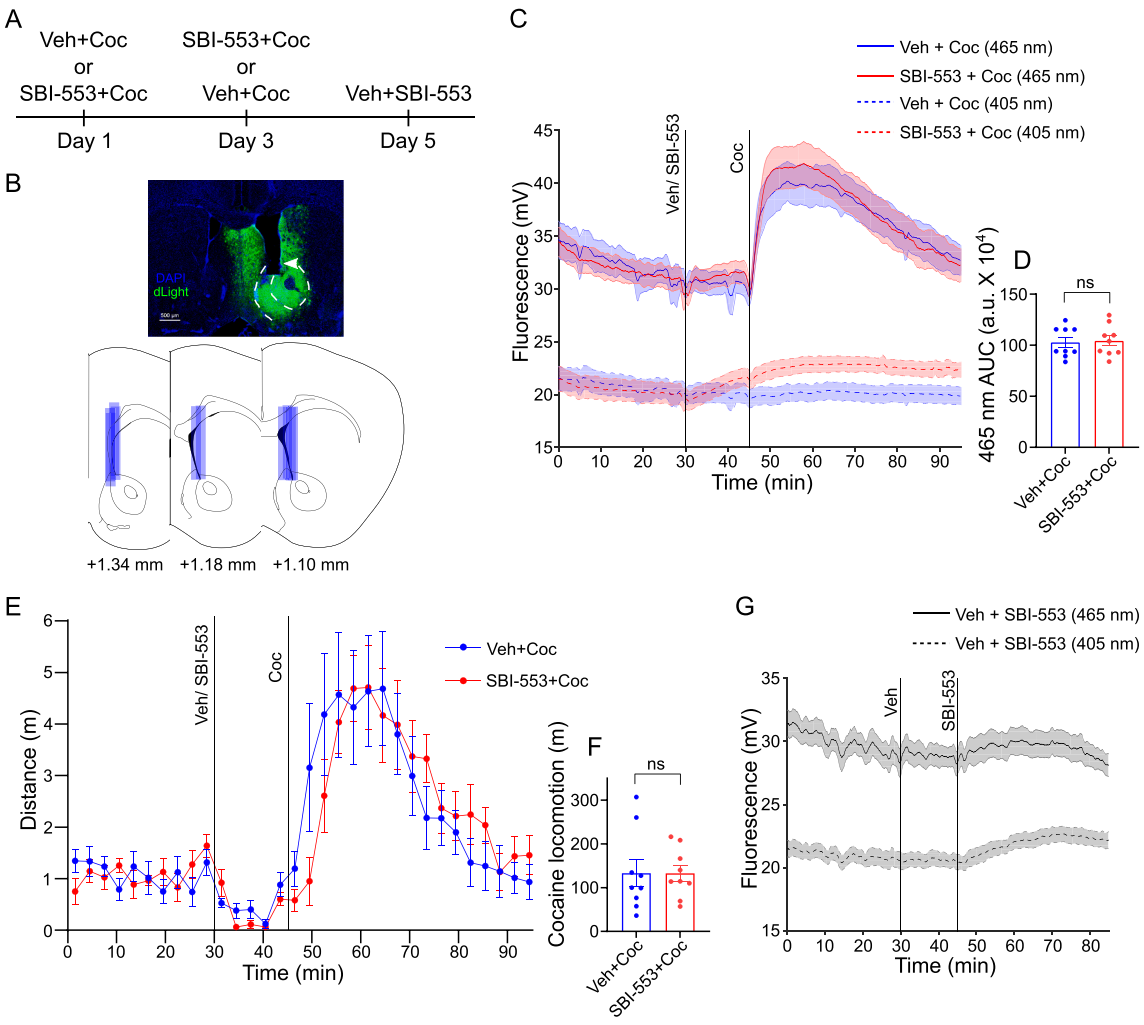

Fig. 4. SBI-553 does not affect basal or cocaine-mediated increase in DA in NAc in vivo. **(A)** Timeline for investigating effects of SBI-553 on basal and cocaine-evoked DA in NAc. **(B)** Coronal section of dLight 1.1 expression in NAc with optic fiber tract (arrowhead); map of optic fiber placements. **(C)** Timecourse of cocaine-potentiated increase in DA fluorescence (465 nm) in NAc, n = 9 mice. **(D)** The cocaine-induced increase in DA was not altered by SBI-553 pre-treatment. AUC (465 nm) was measured from 46 to 90 min; paired *t*-test, p = 0.83, n = 9 mice. **(E)** Timecourse of cocaine-induced hyperlocomotion measured simultaneously in the same mice, n = 9 mice. **(F)** No change in cumulative cocaine-induced locomotion was detected between the vehicle (Veh) and SBI-553 pretreatment groups, AUC was measured from 46 to 90 min; paired *t*-test, p = 0.99, n = 9 mice. **(G)** SBI-553 itself induced a small increase in both 405 nm and 465 nm F, though this was more apparent in the 405 nm signal, n = 10 mice.

antagonizing NT's effects on DA release in NAc through mechanisms similar to those discussed above for VTA.

Despite our *ex vivo* results showing NT-dependent inhibitory effects of SBI-553 on DA neurons, in vivo effects of SBI-553 on DA neuron activity could differ. Indeed, local infusion of NT into the VTA or NAc can elicit different behavioral responses that may reflect distinct actions on pre- or post-synaptic NTR1 across multiple NTR1-expressing cell types. NT infusion or release in to VTA increased DA neuron excitability, DA release in NAc, and locomotor activity, similar to the effects of psychostimulants; conversely NT infusion into NAc reduced psychostimulant-induced hyperactivity or locomotor activity induced by local dopamine injection (Boules et al., 2013; Kalivas et al., 1984; Patterson et al., 2015; Richelson et al., 2003). These region-specific effects may result from NTR1 expression on multiple cell populations. This complexity may also account for why the systemic administration of either NTR1 agonists or NTR1 antagonists have been found to decrease psychostimulant-induced behaviors (Boules et al., 2013; Ferraro et al., 2016; Richelson et al., 2003; Sharpe et al., 2017). Notably, systemic injections of SBI-553 reduced effects of cocaine and methamphetamine on reinforcement and locomotion (Slosky et al., 2020).

Our experiments did not reveal acute effects of SBI-553 on basal or cocaine-evoked DA release in NAc. This finding is in line with the observation that the NTR1 antagonist SR48692 does not alter extracellular DA levels in NAc (Steinberg et al., 1994) and seems to suggest that the behavioral effects of SBI-553 are attributable to circuits downstream of DA release. Such an effect could be in line with the inhibitory action of NT on NAc DA-evoked locomotion (Kalivas et al., 1984). Alternatively, the behavioral effects of SBI-553 may be dependent on plastic changes that occur as a consequence of repeated cocaine exposure. For example, chronic psychostimulants can increase brain NT levels (Betancur et al., 1997; Binder et al., 2001; Torruella-Suárez and McElligott, 2020), thus chronic cocaine could induce changes in endogenous NT signaling that SBI-553 acts to reverse. Indeed, if the actions of SBI-553 on DA neurons are primarily dependent on antagonizing the effects of NT, as we observed in our *ex vivo* experiments, then we may not have observed an in vivo effect of SBI-553 on DA release because of low endogenous NT signaling under the conditions assessed. Future experiments investigating effects of SBI-553 following more chronic treatment regimens are needed to address this.

In the present study, SBI-553 did not inhibit cocaine-induced locomotion, though we observed an apparent delay in the onset of cocaine-induced activity. The inhibitory effects of SBI-553 and its precursor

ML314 on locomotion have been observed in multiple contexts, including in dopamine transporter knock-out mice following i.p. and p.o. administration (Barak et al., 2016; Pinkerton et al., 2019; Slosky et al., 2020), in methamphetamine-induced locomotor paradigms (Barak et al., 2016; Slosky et al., 2020), and in cocaine-induced locomotor paradigms (Slosky et al., 2020). In the current study, several factors deviated from prior paradigms and may contribute to the lack of effect, including that mice received SBI-553 offset by 15 min rather than synchronized with stimulant challenge, that we used a counter-balanced within-subjects design rather than separate cohorts, that mice underwent craniotomy, and that mice were tethered which may limit maximal speed. Future studies could explore these parameters.

We did not specifically observe clear signatures of β-arrestin recruitment by SBI-553 in our experiments, however, several studies highlight the importance of β-arrestin signaling in vivo, including in drug psychomotor activation and reinforcement (Harris and Urs, 2021; Huang et al., 2018; Porter-Stransky and Weinshenker, 2017; Whalen et al., 2011). SBI-553's effects on methamphetamine-induced hyperlocomotion were absent in conditional knockout (cKO) mice lacking β-arrestin2 in striatal D2R-expressing medium spiny neurons (MSNs) and persisted in cKO mice lacking β-arrestin2 in midbrain dopamine neurons (Slosky et al., 2020). However, there is a conspicuous lack of evidence that MSN's express NTR1, and some data suggests that VTA DA cells express β-arrestin1 but not β-arrestin2 (Thibault et al., 2011). To address these questions, future experiments examining the cell-type-specific expression of NT receptors and physiological effects of SBI-553 are needed. Although our experiments focused on the effects of SBI-553 on the mesolimbic DA circuit, NTR1 expression has also been found on glutamate terminals in the striatum (Ferraro et al., 2007, 2008). Indeed, much work implicates glutamate inputs to NAc in addiction and substance use disorders (Buck et al., 2021; D'Souza, 2015; Grueter et al., 2012; Lüscher, 2016; Scofield et al., 2016). Thus, modulation of glutamate release by NT and SBI-553 in the NAc represent a high-priority focus of future studies. NTR1s are also robustly expressed in other brain regions linked to motivated behavior including the septum, hippocampus, amygdala, bed nucleus of stria terminalis (BNST) and hypothalamic nuclei (Boudin et al., 1996; Geisler et al., 2006; Kaneko et al., 2021; Lei and Hu, 2021).

In summary, our current results suggest that SBI-553 inhibits DA neuron activity and release through antagonistic effects on NT-mediated excitation and disinhibition of D2R, most likely by acting as an antagonist of NTR1 G-protein signaling. D2Rs are highly expressed in VTA DA neurons, are key regulators of their excitability and DA transmission in the striatum, and disruption of their function has been shown to alter the reinforcing properties of multiple classes of misused drugs (Beaulieu and Gainetdinov, 2011; de Mei et al., 2009; Ford, 2014). Therefore, effects of SBI-553 on D2R signaling may contribute to its effects on psychostimulant-evoked behaviors.

Funding sources

VA Merit I01BX003759, NIH R01DA036612, NIH R00DA048970, NIH R33DA038019.

CRediT authorship contribution statement

Sarthak M. Singhal: Methodology, Validation, Formal analysis, Investigation, Writing – original draft, Writing – review & editing, Visualization. **Vivien Zell:** Methodology, Formal analysis, Investigation, Writing – review & editing, Visualization. **Lauren Faget:** Software, Formal analysis, Writing – review & editing, Visualization. **Lauren M. Slosky:** Conceptualization, Writing – review & editing. **Lawrence S. Barak:** Conceptualization, Writing – review & editing. **Marc G. Caron:** Conceptualization. **Anthony B. Pinkerton:** Resources. **Thomas S. Hnasko:** Conceptualization, Methodology, Validation, Resources, Writing – review & editing, Visualization, Supervision, Project administration, Funding acquisition.

Declaration of competing interest

US patents 9 868 707 and 10 118 902 relating to the chemistry of SBI-553 and its derivatives have been issued to the Sanford Burnham Prebys Medical Research Institute (A.B·P.) and Duke University (M.G.C., L.S·B.).

Data availability

Data will be made available on request.

References

Alexander, M.J., Leeman, S.E., 1998. Widespread expression in adult rat forebrain of mRNA encoding high-affinity neurotensin receptor. J. Comp. Neurol. 402, 475–500.

Barak, L.S., Bai, Y., Peterson, S., Evron, T., Urs, N.M., Peddibhotla, S., Hedrick, M.P., Hershberger, P., Maloney, P.R., Chung, T.D.Y., Rodriguiz, R.M., Wetsel, W.C., Thomas, J.B., Hanson, G.R., Pinkerton, A.B., Caron, M.G., 2016. ML314: a biased neurotensin receptor ligand for methamphetamine abuse. ACS Chem. Biol. 11, 1880–1890. https://doi.org/10.1021/acschembio.6b00291.

Beaulieu, J.-M., Gainetdinov, R.R., 2011. The physiology, signaling, and pharmacology of dopamine receptors. Pharmacol. Rev. 63, 182–217. https://doi.org/10.1124/pr.110.002642.

Besserer-Offroy, É., Brouillette, R.L., Lavenus, S., Froehlich, U., Brumwell, A., Murza, A., Longpré, J.-M., Marsault, É., Grandbois, M., Sarret, P., Leduc, R., 2017. The signaling signature of the neurotensin type 1 receptor with endogenous ligands. Eur. J. Pharmacol. 805, 1–13. https://doi.org/10.1016/j.ejphar.2017.03.046.

Betancur, C., Rostène, W., Bérod, A., 1997. Chronic cocaine increases neurotensin gene expression in the shell of the nucleus accumbens and in discrete regions of the striatum. Mol. Brain Res. 44, 334–340. https://doi.org/10.1016/S0169-328X(96)00289-6.

Binder, E.B., Kinkead, B., Owens, M.J., Nemeroff, C.B., 2001. Neurotensin and dopamine interactions. Pharmacol. Rev. 53, 453–486.

Boudin, H., Pélaprat, D., Rostène, W., Beaudet, A., 1996. Cellular distribution of neurotensin receptors in rat brain: immunohistochemical study using an antipeptide antibody against the cloned high affinity receptor. J. Comp. Neurol. 373, 76–89. https://doi.org/10.1002/(SICI)1096-9861(19960909)373:1<76::AID-CNE7>3.0.CO;2-A.

Boules, M., Li, Z., Smith, K., Fredrickson, P., Richelson, E., 2013. Diverse roles of neurotensin agonists in the central nervous system. Front. Endocrinol. 4, 36. https://doi.org/10.3389/fendo.2013.00036.

Boules, M.M., Fredrickson, P., Muehlmann, A.M., Richelson, E., 2014. Elucidating the role of neurotensin in the pathophysiology and management of major mental disorders. Behav. Sci. 4, 125–153. https://doi.org/10.3390/bs4020125.

Buck, S.A., Torregrossa, M.M., Logan, R.W., Freyberg, Z., 2021. Roles of dopamine and glutamate co-release in the nucleus accumbens in mediating the actions of drugs of abuse. FEBS J. 288, 1462–1474. https://doi.org/10.1111/febs.15496.

Cáceda, R., Kinkead, B., Nemeroff, C.B., 2006. Neurotensin: role in psychiatric and neurological diseases. Peptides (N.Y.) 27, 2385–2404. https://doi.org/10.1016/j.peptides.2006.04.024.

de Mei, C., Ramos, M., Iitaka, C., Borrelli, E., 2009. Getting specialized: presynaptic and postsynaptic dopamine D2 receptors. Curr. Opin. Pharmacol. 9, 53–58. https://doi.org/10.1016/j.coph.2008.12.002.

Dilts, R.P., Kalivas, P.W., 1989. Autoradiographic localization of mu-opioid and neurotensin receptors within the mesolimbic dopamine system. Brain Res. 488, 311–327. https://doi.org/10.1016/0006-8993(89)90723-3.

D'Souza, M.S., 2015. Glutamatergic transmission in drug reward: implications for drug addiction. Front. Neurosci. 9, 404. https://doi.org/10.3389/fnins.2015.00404.

Fawaz, C.S., Martel, P., Leo, D., Trudeau, L.-E., 2009. Presynaptic action of neurotensin on dopamine release through inhibition of D(2) receptor function. BMC Neurosci. 10, 96. https://doi.org/10.1186/1471-2202-10-96.

Ferraro, L., Tiozzo Fasiolo, L., Beggiato, S., Borelli, A.C., Pomierny-Chamiolo, L., Frankowska, M., Antonelli, T., Tomasini, M.C., Fuxe, K., Filip, M., 2016. Neurotensin: a role in substance use disorder? J. Psychopharmacol. 30, 112–127. https://doi.org/10.1177/0269881115622240.

Ferraro, L., Tomasini, M.C., Fuxe, K., Agnati, L.F., Mazza, R., Tanganelli, S., Antonelli, T., 2007. Mesolimbic dopamine and cortico-accumbens glutamate afferents as major targets for the regulation of the ventral striato-pallidal GABA pathways by neurotensin peptides. Brain Res. Rev. 55, 144–154. https://doi.org/10.1016/j.brainresrev.2007.03.006.

Ferraro, L., Tomasini, M.C., Mazza, R., Fuxe, K., Fournier, J., Tanganelli, S., Antonelli, T., 2008. Neurotensin receptors as modulators of glutamatergic transmission. Brain Res. Rev. 58, 365–373. https://doi.org/10.1016/j.brainresrev.2007.11.001.

Ford, C.P., 2014. The role of D2-autoreceptors in regulating dopamine neuron activity and transmission. Neuroscience 282, 13–22. https://doi.org/10.1016/j.neuroscience.2014.01.025.

Geisler, S., Bérod, A., Zahm, D.S., Rostène, W., 2006. Brain neurotensin, psychostimulants, and stress–emphasis on neuroanatomical substrates. Peptides (N.Y.) 27, 2364–2384. https://doi.org/10.1016/j.peptides.2006.03.037.

Grueter, B.A., Rothwell, P.E., Malenka, R.C., 2012. Integrating synaptic plasticity and striatal circuit function in addiction. Curr. Opin. Neurobiol. 22, 545–551. https://doi.org/10.1016/j.conb.2011.09.009.

Harris, S.S., Urs, N.M., 2021. Targeting β-arrestins in the treatment of psychiatric and neurological disorders. CNS Drugs 35, 253–264. https://doi.org/10.1007/s40263-021-00796-y.

Huang, B., Li, Y., Cheng, D., He, G., Liu, X., Ma, L., 2018. β-Arrestin-biased β-adrenergic signaling promotes extinction learning of cocaine reward memory. Sci. Signal. 11 https://doi.org/10.1126/scisignal.aam5402.

Huang, W., Masureel, M., Qu, Q., Janetzko, J., Inoue, A., Kato, H.E., Robertson, M.J., Nguyen, K.C., Glenn, J.S., Skiniotis, G., Kobilka, B.K., 2020. Structure of the neurotensin receptor 1 in complex with β-arrestin 1. Nature 579, 303–308. https://doi.org/10.1038/s41586-020-1953-1.

Jomphe, C., Lemelin, P.-L., Okano, H., Kobayashi, K., Trudeau, L.-E., 2006. Bidirectional regulation of dopamine D2 and neurotensin NTS1 receptors in dopamine neurons. Eur. J. Neurosci. 24, 2789–2800. https://doi.org/10.1111/j.1460-9568.2006.05151.x.

Kalivas, P.W., Nemeroff, C.B., Prange, A.J., 1984. Neurotensin microinjection into the nucleus accumbens antagonizes dopamine-induced increase in locomotion and rearing. Neuroscience 11, 919–930. https://doi.org/10.1016/0306-4522(84)90203-3.

Kaneko, T., Hara, R., Amano, T., Minami, M., 2021. Diverse intracellular signaling pathways mediate the effects of neurotensin on the excitability of type II neurons in the rat dorsolateral bed nucleus of the stria terminalis. J. Pharmacol. Sci. 147, 86–94. https://doi.org/10.1016/j.jphs.2021.05.013.

Legault, M., Congar, P., Michel, F.J., Trudeau, L.-E., 2002. Presynaptic action of neurotensin on cultured ventral tegmental area dopaminergic neurones. Neuroscience 111, 177–187. https://doi.org/10.1016/s0306-4522(01)00614-5.

Lei, S., Hu, B., 2021. Ionic and signaling mechanisms involved in neurotensin-mediated excitation of central amygdala neurons. Neuropharmacology 196, 108714. https://doi.org/10.1016/j.neuropharm.2021.108714.

Lüscher, C., 2016. The emergence of a circuit model for addiction. Annu. Rev. Neurosci. 39, 257–276. https://doi.org/10.1146/annurev-neuro-070815-013920.

Palacios, J.M., Kuhar, M.J., 1981. Neurotensin receptors are located on dopamine-containing neurones in rat midbrain. Nature 294, 587–589. https://doi.org/10.1038/294587a0.

Patterson, C.M., Wong, J.-M.T., Leinninger, G.M., Allison, M.B., Mabrouk, O.S., Kasper, C.L., Gonzalez, I.E., Mackenzie, A., Jones, J.C., Kennedy, R.T., Myers, M.G., 2015. Ventral tegmental area neurotensin signaling links the lateral hypothalamus to locomotor activity and striatal dopamine efflux in male mice. Endocrinology 156, 1692–1700. https://doi.org/10.1210/en.2014-1986.

Pettibone, D.J., Hess, J.F., Hey, P.J., Jacobson, M.A., Leviten, M., Lis, E. v, Mallorga, P.J., Pascarella, D.M., Snyder, M.A., Williams, J.B., Zeng, Z., 2002. The effects of deleting the mouse neurotensin receptor NTR1 on central and peripheral responses to neurotensin. J. Pharmacol. Exp. Therapeut. 300, 305–313. https://doi.org/10.1124/jpet.300.1.305.

Phillips, P.E.M., Hancock, P.J., Stamford, J.A., 2002. Time window of autoreceptor-mediated inhibition of limbic and striatal dopamine release. Synapse 44, 15–22. https://doi.org/10.1002/syn.10049.

Piccart, E., Courtney, N.A., Branch, S.Y., Ford, C.P., Beckstead, M.J., 2015. Neurotensin induces presynaptic depression of D2 dopamine autoreceptor-mediated neurotransmission in midbrain dopaminergic neurons. J. Neurosci. 35, 11144–11152. https://doi.org/10.1523/JNEUROSCI.3816-14.2015.

Pickel, V.M., Chan, J., Delle Donne, K.T., Boudin, H., Pélaprat, D., Rosténe, W., 2001. High-affinity neurotensin receptors in the rat nucleus accumbens: subcellular targeting and relation to endogenous ligand. J. Comp. Neurol. 435, 142–155. https://doi.org/10.1002/cne.1198.

Pinkerton, A.B., Peddibhotla, S., Yamamoto, F., Slosky, L.M., Bai, Y., Maloney, P., Hershberger, P., Hedrick, M.P., Falter, B., Ardecky, R.J., Smith, L.H., Chung, T.D.Y., Jackson, M.R., Caron, M.G., Barak, L.S., 2019. Discovery of β-arrestin biased, orally bioavailable, and CNS penetrant neurotensin receptor 1 (NTR1) allosteric modulators. J. Med. Chem. 62, 8357–8363. https://doi.org/10.1021/acs.jmedchem.9b00340.

Porter-Stransky, K.A., Weinshenker, D., 2017. Arresting the development of addiction: the role of β-arrestin 2 in drug abuse. J. Pharmacol. Exp. Therapeut. 361, 341–348. https://doi.org/10.1124/jpet.117.240622.

Quirion, R., Chiueh, C.C., Everist, H.D., Pert, A., 1985. Comparative localization of neurotensin receptors on nigrostriatal and mesolimbic dopaminergic terminals. Brain Res. 327, 385–389. https://doi.org/10.1016/0006-8993(85)91542-2.

Reiter, E., Ahn, S., Shukla, A.K., Lefkowitz, R.J., 2012. Molecular mechanism of β-arrestin-biased agonism at seven-transmembrane receptors. Annu. Rev. Pharmacol. Toxicol. 52, 179–197. https://doi.org/10.1146/annurev.pharmtox.010909.105800.

Remaury, A., Vita, N., Gendreau, S., Jung, M., Arnone, M., Poncelet, M., Culouscou, J.-M., le Fur, G., Soubrié, P., Caput, D., Shire, D., Kopf, M., Ferrara, P., 2002. Targeted inactivation of the neurotensin type 1 receptor reveals its role in body temperature control and feeding behavior but not in analgesia. Brain Res. 953, 63–72. https://doi.org/10.1016/s0006-8993(02)03271-7.

Reyneke, L., Russell, V.A., Taljaard, J.J., 1992. Regional effects of neurotensin on the electrically stimulated release of [3H]dopamine and [14C]acetylcholine in the rat nucleus accumbens. Neurochem. Res. 17, 1143–1146. https://doi.org/10.1007/BF00967292.

Richelson, E., Boules, M., Fredrickson, P., 2003. Neurotensin agonists: possible drugs for treatment of psychostimulant abuse. Life Sci. 73, 679–690. https://doi.org/10.1016/s0024-3205(03)00388-6.

Sarret, P., Beaudet, A., Vincent, J.P., Mazella, J., 1998. Regional and cellular distribution of low affinity neurotensin receptor mRNA in adult and developing mouse brain. J. Comp. Neurol. 394, 344–356.

Schotte, A., Leysen, J.E., 1989. Autoradiographic evidence for the localization of high affinity neurotensin binding sites on dopaminergic nerve terminals in the nigrostriatal and mesolimbic pathways in rat brain. J. Chem. Neuroanat. 2, 253–257.

Schroeder, L.E., Furdock, R., Quiles, C.R., Kurt, G., Perez-Bonilla, P., Garcia, A., Colon-Ortiz, C., Brown, J., Bugescu, R., Leinninger, G.M., 2019. Mapping the populations of neurotensin neurons in the male mouse brain. Neuropeptides 76, 101930. https://doi.org/10.1016/j.npep.2019.05.001.

Scofield, M.D., Heinsbroek, J.A., Gipson, C.D., Kupchik, Y.M., Spencer, S., Smith, A.C.W., Roberts-Wolfe, D., Kalivas, P.W., 2016. The nucleus accumbens: mechanisms of addiction across drug classes reflect the importance of glutamate homeostasis. Pharmacol. Rev. 68, 816–871. https://doi.org/10.1124/pr.116.012484.

Sharpe, A.L., Varela, E., Beckstead, M.J., 2017. Systemic PD149163, a neurotensin receptor 1 agonist, decreases methamphetamine self-administration in DBA/2J mice without causing excessive sedation. PLoS One 12, e0180710. https://doi.org/10.1371/journal.pone.0180710.

Shi, W.X., Bunney, B.S., 1992. Roles of intracellular cAMP and protein kinase A in the actions of dopamine and neurotensin on midbrain dopamine neurons. J. Neurosci. 12, 2433–2438.

Shin, J.H., Adrover, M.F., Alvarez, V.A., 2017. Distinctive modulation of dopamine release in the nucleus accumbens shell mediated by dopamine and acetylcholine receptors. J. Neurosci. 37, 11166–11180. https://doi.org/10.1523/JNEUROSCI.0596-17.2017.

Slosky, L.M., Bai, Y., Toth, K., Ray, C., Rochelle, L.K., Badea, A., Chandrasekhar, R., Pogorelov, V.M., Abraham, D.M., Atluri, N., Peddibhotla, S., Hedrick, M.P., Hershberger, P., Maloney, P., Yuan, H., Li, Z., Wetsel, W.C., Pinkerton, A.B., Barak, L.S., Caron, M.G., 2020. β-Arrestin-Biased allosteric modulator of NTSR1 selectively attenuates addictive behaviors. Cell 181, 1364–1379. https://doi.org/10.1016/j.cell.2020.04.053 e14.

Smith, J.S., Rajagopal, S., 2016. The β-arrestins: multifunctional regulators of G protein-coupled receptors. J. Biol. Chem. 291, 8969–8977. https://doi.org/10.1074/jbc.R115.713313.

Steinberg, R., Brun, P., Fournier, M., Souilhac, J., Rodier, D., Mons, G., Terranova, J.P., le Fur, G., Soubrié, P., 1994. SR 48692, a non-peptide neurotensin receptor antagonist differentially affects neurotensin-induced behaviour and changes in dopaminergic transmission. Neuroscience 59, 921–929. https://doi.org/10.1016/0306-4522(94)90295-X.

St-Gelais, F., Jomphe, C., Trudeau, L.-E., 2006. The role of neurotensin in central nervous system pathophysiology: what is the evidence? J. Psychiatry Neurosci. 31, 229–245.

St-Gelais, F., Legault, M., Bourque, M.-J., Rompré, P.-P., Trudeau, L.-E., 2004. Role of calcium in neurotensin-evoked enhancement in firing in mesencephalic dopamine neurons. J. Neurosci. 24, 2566–2574. https://doi.org/10.1523/JNEUROSCI.5376-03.2004.

Stuhrman, K., Roseberry, A.G., 2015. Neurotensin inhibits both dopamine- and GABA-mediated inhibition of ventral tegmental area dopamine neurons. J. Neurophysiol. 114, 1734–1745. https://doi.org/10.1152/jn.00279.2015.

Thibault, D., Albert, P.R., Pineyro, G., Trudeau, L.-É., 2011. Neurotensin triggers dopamine D2 receptor desensitization through a protein kinase C and beta-arrestin1-dependent mechanism. J. Biol. Chem. 286, 9174–9184. https://doi.org/10.1074/jbc.M110.166454.

Ting, J.T., Lee, B.R., Chong, P., Soler-Llavina, G., Cobbs, C., Koch, C., Zeng, H., Lein, E., 2018. Preparation of acute brain slices using an optimized N-Methyl-D-glucamine protective recovery method. J. Vis. Exp. https://doi.org/10.3791/53825.

Torruella-Suárez, M.L., McElligott, Z.A., 2020. Neurotensin in reward processes. Neuropharmacology 167, 108005. https://doi.org/10.1016/j.neuropharm.2020.108005.

Tschumi, C.W., Beckstead, M.J., 2019. Diverse actions of the modulatory peptide neurotensin on central synaptic transmission. Eur. J. Neurosci. 49, 784–793. https://doi.org/10.1111/ejn.13858.

Tschumi, C.W., Blankenship, H.E., Sharma, R., Lynch, W.B., Beckstead, M.J., 2022. Neurotensin release from dopamine neurons drives long-term depression of substantia nigra dopamine signaling. J. Neurosci. 42, 6186–6194. https://doi.org/10.1523/JNEUROSCI.1395-20.2022.

von Euler, G., van der Ploeg, I., Fredholm, B.B., Fuxe, K., 1991. Neurotensin decreases the affinity of dopamine D2 agonist binding by a G protein-independent mechanism. J. Neurochem. 56, 178–183. https://doi.org/10.1111/j.1471-4159.1991.tb02578.x.

Werkman, T.R., Kruse, C.G., Nievelstein, H., Long, S.K., Wadman, W.J., 2000. Neurotensin attenuates the quinpirole-induced inhibition of the firing rate of dopamine neurons in the rat substantia nigra pars compacta and the ventral tegmental area. Neuroscience 95, 417–423. https://doi.org/10.1016/s0306-4522(99)00449-2.

Whalen, E.J., Rajagopal, S., Lefkowitz, R.J., 2011. Therapeutic potential of β-arrestin- and G protein-biased agonists. Trends Mol. Med. 17, 126–139. https://doi.org/10.1016/j.molmed.2010.11.004.

Woodworth, H.L., Batchelor, H.M., Beekly, B.G., Bugescu, R., Brown, J.A., Kurt, G., Fuller, P.M., Leinninger, G.M., 2017. Neurotensin receptor-1 identifies a subset of ventral tegmental dopamine neurons that coordinates energy balance. Cell Rep. 20, 1881–1892. https://doi.org/10.1016/j.celrep.2017.08.001.

Woodworth, H.L., Brown, J.A., Batchelor, H.M., Bugescu, R., Leinninger, G.M., 2018a. Determination of neurotensin projections to the ventral tegmental area in mice. Neuropeptides 68, 57–74. https://doi.org/10.1016/j.npep.2018.02.003.

Woodworth, H.L., Perez-Bonilla, P.A., Beekly, B.G., Lewis, T.J., Leinninger, G.M., 2018b. Identification of neurotensin receptor expressing cells in the ventral tegmental area across the lifespan. eNeuro 5. https://doi.org/10.1523/ENEURO.0191-17.2018.